JACS JOURNAL OF THE AMERICAN CHEMICAL SOCIETY

Article

Cite This: J. Am. Chem. Soc. 2018, 140, 16544−16552

pubs.acs.org/JACS

Enforcing Extended Porphyrin J-Aggregate Stacking in Covalent Organic Frameworks

Niklas Keller,[†] Mona Calik,[†] Dmitry Sharapa,[‡] Himadri R. Soni,[§,¶] Peter M. Zehetmaier,[†] Sabrina Rager,[†] Florian Auras,[∥] Andreas C. Jakowetz,[†] Andreas Görling,[§] Timothy Clark,[‡] and Thomas Bein*[,†]

[†]Department of Chemistry and Center for NanoScience (CeNS), University of Munich (LMU), Butenandtstrasse 5-13, 81377 Munich, Germany

[‡]Computer-Chemie-Centrum and Interdisciplinary Center for Molecular Materials, Friedrich-Alexander-Universität Erlangen-Nürnberg, Nägelsbachstraße 25, 91052 Erlangen, Germany

[§]Chair of Theoretical Chemistry, Friedrich-Alexander-Universität Erlangen-Nürnberg (FAU), Egerlandstraße 3, 91058 Erlangen, Germany

[∥]Cavendish Laboratory, University of Cambridge, JJ Thomson Avenue, Cambridge CB3 0HE, United Kingdom

Supporting Information

ABSTRACT: The potential of covalent organic frameworks (COFs) for realizing porous, crystalline networks with tailored combinations of functional building blocks has attracted considerable scientific interest in the fields of gas storage, photocatalysis, and optoelectronics. Porphyrins are widely studied in biology and chemistry and constitute promising building blocks in the field of electroactive materials, but they reveal challenges regarding crystalline packing when introduced into COF structures due to their nonplanar configuration and strong electrostatic interactions between the heterocyclic porphyrin centers. A series of porphyrin-containing imine-linked COFs with linear bridges derived from terephthalaldehyde, 2,5-dimethoxybenzene-1,4-dicarboxaldehyde, 4,4′-biphenyldicarboxaldehyde and thieno[3,2-*b*]thiophene-2,5-dicarboxaldehyde, were synthesized, and their structural and optical properties were examined. By combining X-ray diffraction analysis with density-functional theory (DFT) calculations on multiple length scales, we were able to elucidate the crystal structure of the newly synthesized porphyrin-based COF containing thieno[3,2-*b*]thiophene-2,5-dicarboxaldehyde as linear bridge. Upon COF crystallization, the porphyrin nodes lose their 4-fold rotational symmetry, leading to the formation of extended slipped J-aggregate stacks. Steady-state and time-resolved optical spectroscopy techniques confirm the realization of the first porphyrin J-aggregates on a > 50 nm length scale with strongly red-shifted Q-bands and increased absorption strength. Using the COF as a structural template, we were thus able to force the porphyrins into a covalently embedded J-aggregate arrangement. This approach could be transferred to other chromophores; hence, these COFs are promising model systems for applications in photocatalysis and solar light harvesting, as well as for potential applications in medicine and biology.

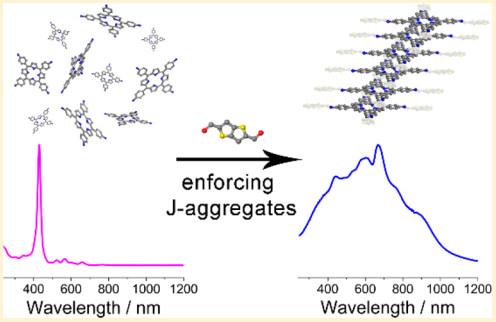

INTRODUCTION

Inspired by numerous natural examples, the self-assembly of molecules has attracted increasing attention as these evolving aggregates often exhibit unique electronic and spectroscopic characteristics. For example, self-assembled derivatives of tetrapyrrole macrocycles of the porphyrin family are of vital importance for natural light-harvesting and electron transfer processes. Thus, understanding and controlling the aggregation of supramolecular structures enables important insights in natural processes such as photosynthesis and in the context of synthetic optoelectronic systems including organic photovoltaics or photodynamic therapy (PDT).[1,2] Here, molecular assembly leads to emergent new features compared to the monomers such as excitonic coupling,[3] photoinduced electron transfer,[4] nonlinear optics,[5] and activation of molecular oxygen.[6,7]

In addition to their enormous importance in natural systems, their extended π-electron system and semiconducting and photoconducting capabilities make porphyrins the most widely studied conjugated macrocycles.[5,8−11] They exhibit high extinction coefficients in the visible and near-infrared (NIR) regions, where the maximum of the solar flux occurs, rendering them interesting candidates for solar light-harvesting.[12] Moreover, porphyrins can act as model systems in medicine and biology due to their close relationship to structures such as

Received: July 30, 2018
Published: November 3, 2018

DOI: 10.1021/jacs.8b08088
J. Am. Chem. Soc. 2018, 140, 16544−16552

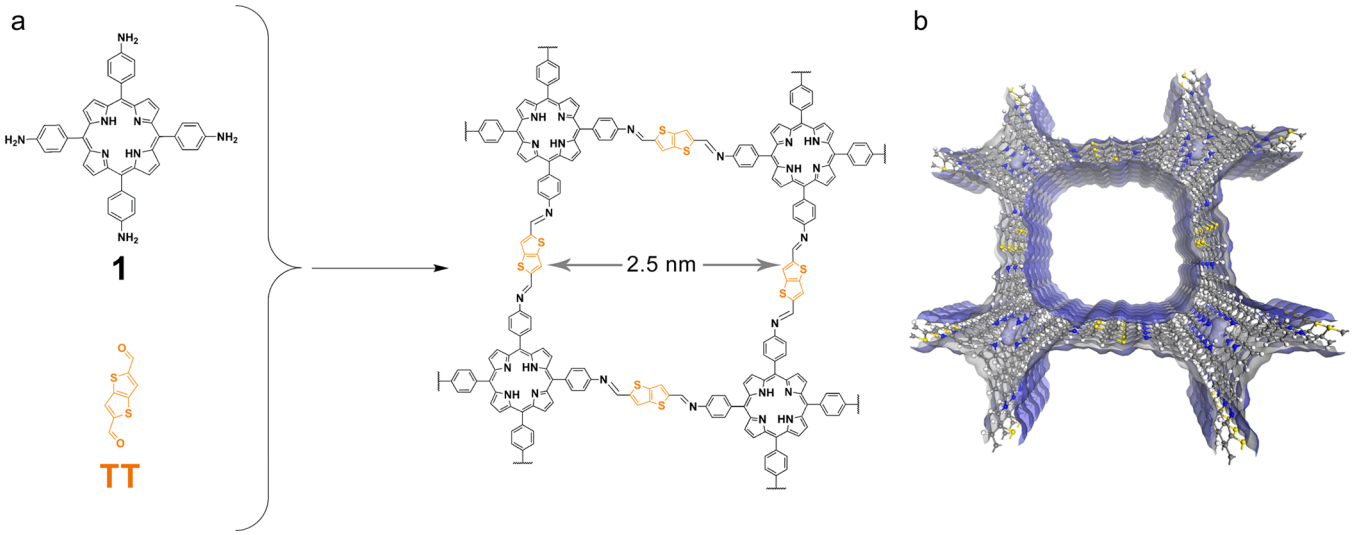

Figure 1. (a) Co-condensation reaction of 5,10,15,20−tetrakis(4-aminophenyl)porphyrin (**1**) and thieno[3,2-*b*]thiophene-2,5-dicarboxaldehyde (TT) in a 1:2 molar ratio to form the TT-Por COF, featuring tetragonal pores with a diameter of 2.5 nm. (b) Illustration of the TT-Por COF, showing the extended, 3-dimensional structure along the *c*-axis.

heme and chlorophyll. The latter is found in light-harvesting complexes present in plants and bacteria.[13−16]

Artificial aggregates of porphyrins have been the focus of many studies, and H-aggregates as well as J-aggregates have been obtained. While both types exhibit a parallel stacking of monomers, in H-aggregates, the monomer centers are aligned on top of each other. In contrast, the centers are offset in a "head-to-tail" fashion in J-aggregates. The resulting aggregate transition dipole moment, taking into account the possible parallel or antiparallel dipole moments on the individual monomers, is shifted to higher (H-type) or lower (J-type) energies, as described in the literature.[17−19] Therefore, controlling the stacking can directly influence the optical properties of a material. So far porphyrin J-aggregates have been synthesized as thin molecular films or dispersed in solutions (dependent on pH), thus limiting the versatility.[20−22] In principle, this issue could be overcome by fixing chromophores in a solid matrix in a highly ordered structure, hence enforcing the system to aggregate in the desired fashion.

Here, we address this challenge by integrating two photoactive units, a tetragonal aminophenyl porphyrin linked to a thieno[3,2-*b*]thiophene-2,5-dicarboxaldehyde (TT) unit, through chemical bonds into a covalent organic framework. To the best of our knowledge, this is the first report on such an ordered porphyrin J-aggregate embedded in a solid matrix with novel optical characteristics, especially in the NIR region, that have not been observed with porphyrins to date. In contrast, H-aggregate formation has been observed in the porphyrin-containing COF-366 (see below).[23] Through targeted selection of molecular units, our synthetic strategy presents a new paradigm for creating highly crystalline solid-state J-aggregates, directed through the structural templating power of a covalent molecular framework.

Ordered in a COF structure, the combination of the above two building blocks leads to a reduction in local symmetry, which is caused by a staircase-like stacking behavior of the porphyrin-COF that causes a splitting of reflections in the X-ray diffraction pattern. This stacking motif results in the strong J-aggregate behavior within the porphyrin stack, which is locked by the surrounding framework structure and drastically changes the optoelectronic properties of the porphyrin moiety. The Q-bands in the absorption spectrum are not only red-shifted compared to the monomer in solution but also gain in transition dipole moment compared to the Soret band, while at the same time the fluorescence lifetime is strongly enhanced as compared to molecular porphyrin crystals.

The extended lattices of highly ordered and tightly packed chromophores in COFs combine novel optical behavior with the unique molecular accessibility of the porous network. Both are promising properties for applications in photovoltaic cells, optoelectronic devices, and could also be of great interest for chemical, medical, and biological applications.[24] For example, photodynamic therapy in medicine could be strongly enhanced by the nonlinear multiphoton absorption of aggregated chromophores and the open architecture of frameworks enabling the efficient conversion of $^3O_2$ to $^1O_2$ at the reactive porphyrin centers.

RESULTS AND DISCUSSION

The new 2D TT-Por COF was synthesized by combining 5,10,15,20−tetrakis(4-aminophenyl)porphyrin (**1**) with thieno[3,2-*b*]thiophene-2,5-dicarboxaldehyde (TT) in a 1:2 molar ratio. The solvothermal reaction was carried out in a solvent mixture of benzyl alcohol, dichlorobenzene and 6 molar acetic acid (30:10:4, *v*:*v*:*v*) for 3 days at 120 °C, identified to be the optimal conditions following comprehensive screening of reaction parameters (Figure 1a; for experimental data, see the Supporting Information (SI)). The porphyrin units, located at the corners, are linked by the linear TT to form an ordered structure with open channels (Figure 1b).

Porphyrins have been integrated into various COF structures.[25−35] The resulting frameworks, with metallo- as well as free-base porphyrins, were found to exhibit an eclipsed structure, meaning that the 2D sheets lie on top of each other in an AA-stacking arrangement, while AB-stacking simulations did not agree with the experimental XRD patterns.[23,36−41] However, density-functional theory (DFT) calculations performed by different groups suggest that truly eclipsed structures are energetically disfavored in most frameworks and

DOI: 10.1021/jacs.8b08088
J. Am. Chem. Soc. 2018, 140, 16544−16552

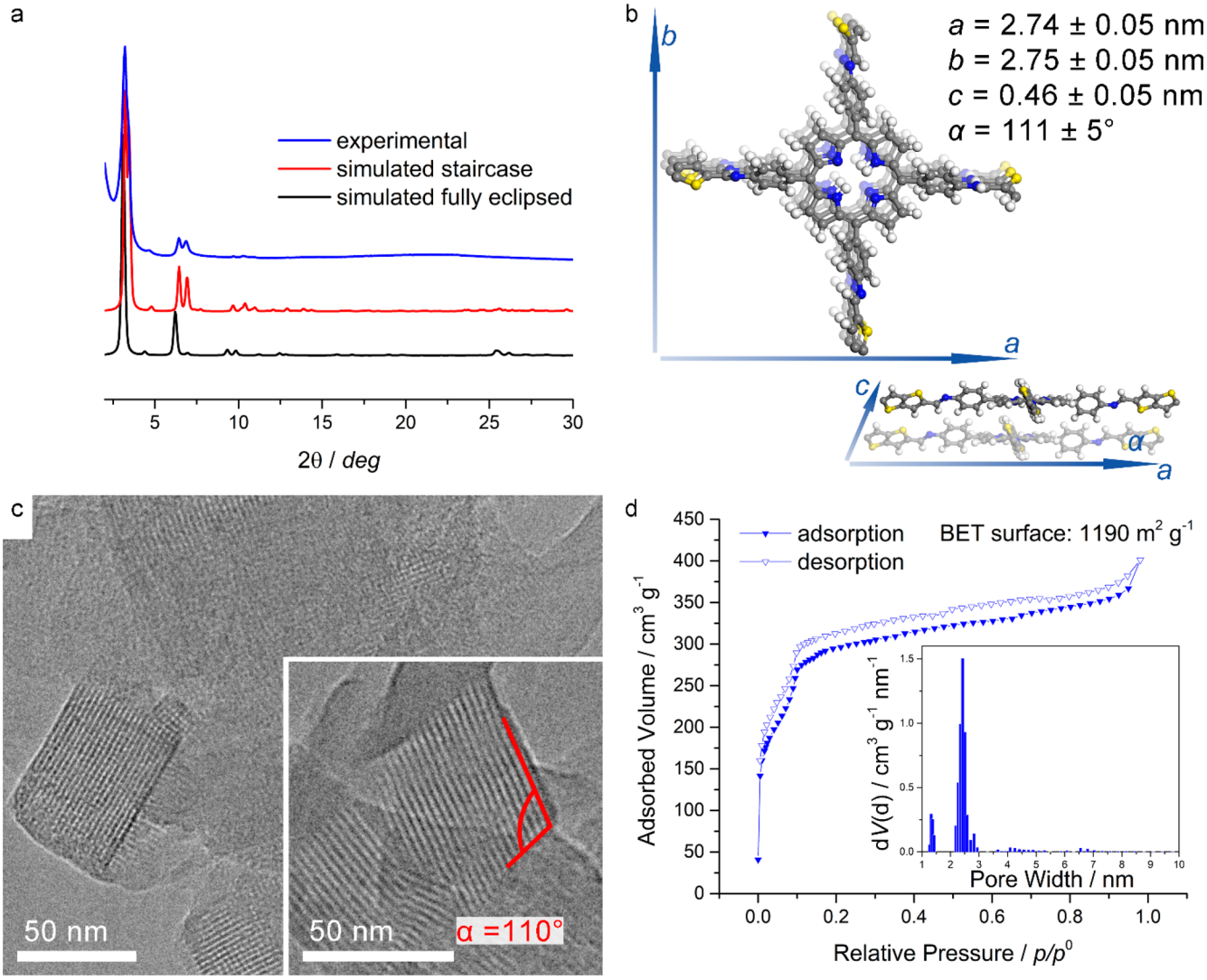

Figure 2. (a) Experimental PXRD data (blue) vs simulated patterns (red and black) for a fully eclipsed and (b) staircase arrangement of the 2D layers of TT-Por COF calculated by AM1. The theoretical XRD patterns were simulated for a crystallite size of 50 nm. (c) Transmission electron micrographs of TT-Por COF bulk material showing the rectangular pore structure with defined crystal facets (bottom left) and the staircase arrangement of the COF with an angle between adjacent layers of 110° (inset bottom right). (d) Nitrogen sorption isotherm of a TT-Por COF powder sample measured at 77 K. The corresponding pore size distribution (inset) with an average pore size of 2.4 nm was obtained by fitting the experimental data using an NLDFT adsorption branch model.

that COFs rather adopt structures with slightly offset layers.[42−44]

In a two-layer system, the offset can occur with the same probability in all symmetry-equivalent directions. However, only if the geometric conformation of this initial bilayer can be conveyed to the growing framework, translational symmetry is generated throughout the COF domain and can be observed via diffraction techniques.[45] While synchronizing the layer offset has become a very effective COF construction principle with C_2-symmetric building blocks,[45−47] this has not been observed experimentally for building blocks of higher rotational symmetry.[42] In the case of the C_4-symmetric tetraphenyl porphyrin, generating an offset-stacked translational symmetry would require breaking the rotational symmetry of each porphyrin node.

Powder X-ray diffraction (PXRD) measurements of the synthesized bulk material confirmed the formation of a crystalline porphyrin COF. To identify the structure, the calculated pattern of an eclipsed P_4-symmetric AA-stacking arrangement was compared to experimental data but did not match (Figure 2a). The size of the unit cell, given by the position of the 100 reflection, however, is in good agreement with the experimental data, suggesting only slight deviations in the unit cell. Both a shoulder on the 100 reflection and a splitting of the 200 reflection into two new distinct peaks indicate a loss in symmetry of the unit cell. Optimizing the geometry, including all unit cell parameters and using a periodic force-field treatment resulted in a simulated pattern that matches the experimental one. In order to produce the correct pattern without neglecting the geometry of the building blocks, the unit cell parameter γ must deviate from 90°, resulting in an offset of the adjacent layers (Figure 2a,b). This offset results in a staircase-like stacking behavior, which is prevalent in one direction and can be distinctly recognized in the PXRD pattern (Figure 2a).

Computer simulations were performed at three different levels of theory: DFT to obtain accurate intermolecular interactions, semiempirical molecular-orbital theory on large

DOI: 10.1021/jacs.8b08088
J. Am. Chem. Soc. 2018, 140, 16544−16552

periodic systems to investigate bulk electronic properties, and molecular mechanics (classical force field) simulations to compute X-ray diffraction patterns for large models to compare with experimental data.

Periodic DFT calculations were carried out with the VASP[48] code. The calculations employed the semilocal exchange-correlation functional due to Perdew, Burke, and Ernzerhof[49] supplemented with the D3 van der Waals correction[50] (including Becke–Johnson damping[51]) to take into account dispersion interactions, see the SI for further details. The unit cell as well as the positions of all atoms within the unit cell were optimized starting from the geometry obtained from AM1 calculations (see below). The obtained lattice parameters, see Table S1 of the SI, are in very good agreement with the XRD data and confirm the suggested staircase geometry. To examine whether other geometries represent local energy minima, we flipped the thiophene units bridging porphyrin rings in the obtained structure and reoptimized again. This optimization, however, led back to the same structure as before.

In order to identify the driving force for creating the staircase geometry, we carried out a geometry optimization in which the interlayer spacing of the COFs was initially set to 15 Å and the unit cell volume was kept fixed. This way the structure of an isolated COF sheet could relax while the interlayer spacing remained at a large distance such that the COF sheets remained isolated. It turned out that in an isolated COF sheet the lateral, i.e., in-plane, unit cell is almost perfectly quadratic with in-plane unit cell vectors of length a = 27.39 Å and b = 27.33 Å and an angle γ = 90.97° between them, see Table S4 of the SI. In the crystalline three-dimensional (3D) material the corresponding in-plane geometry data are a = 27.41 Å, b = 27.46 Å, and γ = 94.34° and an offset angle of α = 111.41°, see Table S1 of the SI. These results show that the formation of the staircase geometry goes along with a certain distortion of the quadratic lateral unit cell of an isolated single sheet of the COF. The calculated formation energy of the 3D material with respect to single sheets is 1.81 eV per unit cell (compare total energies of three-dimensional crystalline material and single sheets, Tables S1 and S4 of the SI) with a van der Waals contribution of 2.13 eV. The finding that the van der Waals contribution to the formation energy is higher than the total formation energy means that packing effects lead to distortions that lower the covalent binding energy of the COF network. This raising of the energy upon formation of the 3D-material is, however, overcompensated by van der Waals interactions. This identifies the latter as the driving force for the formation of the observed staircase structure.

In the periodic semiempirical calculations the MNDO,[52,53] MNDO/d,[54] AM1,[55] and AM1*[56] Hamiltonians were tested with and without Grimme D3-dispersion corrections[50] using the EMPIRE program.[57,58] Minimal unit cells and supercells up to 2 × 2 × 4 (>1600 atoms) were used in the simulations. AM1 was found to be most reliable, correctly describing that aromatic delocalization and π–π stacking are preferred to hydrogen-bond formation. The Grimme corrections are very important for reproducing the interlayer distance and for the energy difference between the eclipsed and staircase arrangements. Several different staircase stacking-patterns were found, including one with unit cell parameters very close to those observed experimentally, while eclipsed stacking was not found to be stable with any of the Hamiltonians investigated. Optimized geometries and unit cell parameters can be found in the SI, Table S1.

A periodic system with 1000 unit cells was subjected to force-field-based simulated annealing (for details, see the SI). This procedure resulted in significantly distorted layers, which, however, retained the staircase shifted pattern. PXRD patterns predicted for idealized and annealed supercells (see the SI for details) fit the experimental curve very well (Figure 3).

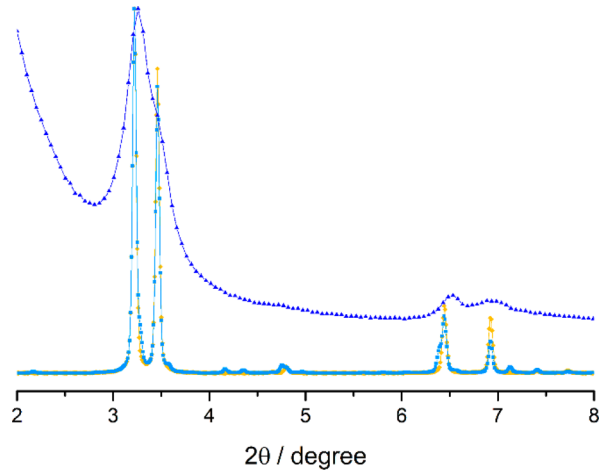

Figure 3. Experimental (blue) and calculated PXRD patterns, ideal (yellow) and annealed (light blue).

The transmission electron microscopy (TEM) images of the TT-Por COF confirmed the successful formation of a crystalline and ordered material. Domain sizes of up to 100 nm and the formation of defined rectangular crystal facets could be observed (Figure 2c). Depending on the orientation of the crystallites, the rectangular porous network can be seen from the top or the porous channels from the side. Some facets are oriented such that the staircase stacking arrangement of the sheets is evident and can directly be seen (Figure 2c, inset bottom right). The measured angle between the adjacent layers is 110° which is in excellent agreement with the angle of 111.41° in the DFT-simulated structure (compare Figure 2b,c, see the SI, Table S1).

Nitrogen sorption measurements reveal the typical shape of a type IV isotherm with a steep increase in adsorbed volume at 0.09 p/p_0 (Figure 2d). The calculated Brunauer–Emmett–Teller (BET) surface area is 1190 $m^2\ g^{-1}$ with a pore volume of 0.56 $cm^3\ g^{-1}$. This corresponds to 57% of the predicted Connolly surface of 2095 $m^2\ g^{-1}$, which can be possibly explained by defects, displacement of COF layers or adsorbed molecular fragments. Nevertheless, similar surface areas have been reported for other porphyrin-containing COFs (see the SI for more details).[23] The pore size shows a very narrow distribution with an average pore size of 2.4 nm (Figure 2d inset) with a fitting error of 0.7%. This is in good agreement with the theoretical pore size of 2.5 nm.

The newly synthesized TT-Por COF shows a strong absorbance throughout the UV and visible spectral range, tailing far into the infrared region with distinct features (Figure 4a, blue). Peak absorption is at 668 nm with two more distinct peaks at 444 and 600 nm. The peak at 444 nm corresponds to the Soret band ($S_2 \leftarrow S_0$), as it can be easily observed in the absorption spectrum of porphyrin monomers in solution (Figure 4b). The two peaks at 600 and 668 nm can be

DOI: 10.1021/jacs.8b08088
J. Am. Chem. Soc. 2018, 140, 16544–16552

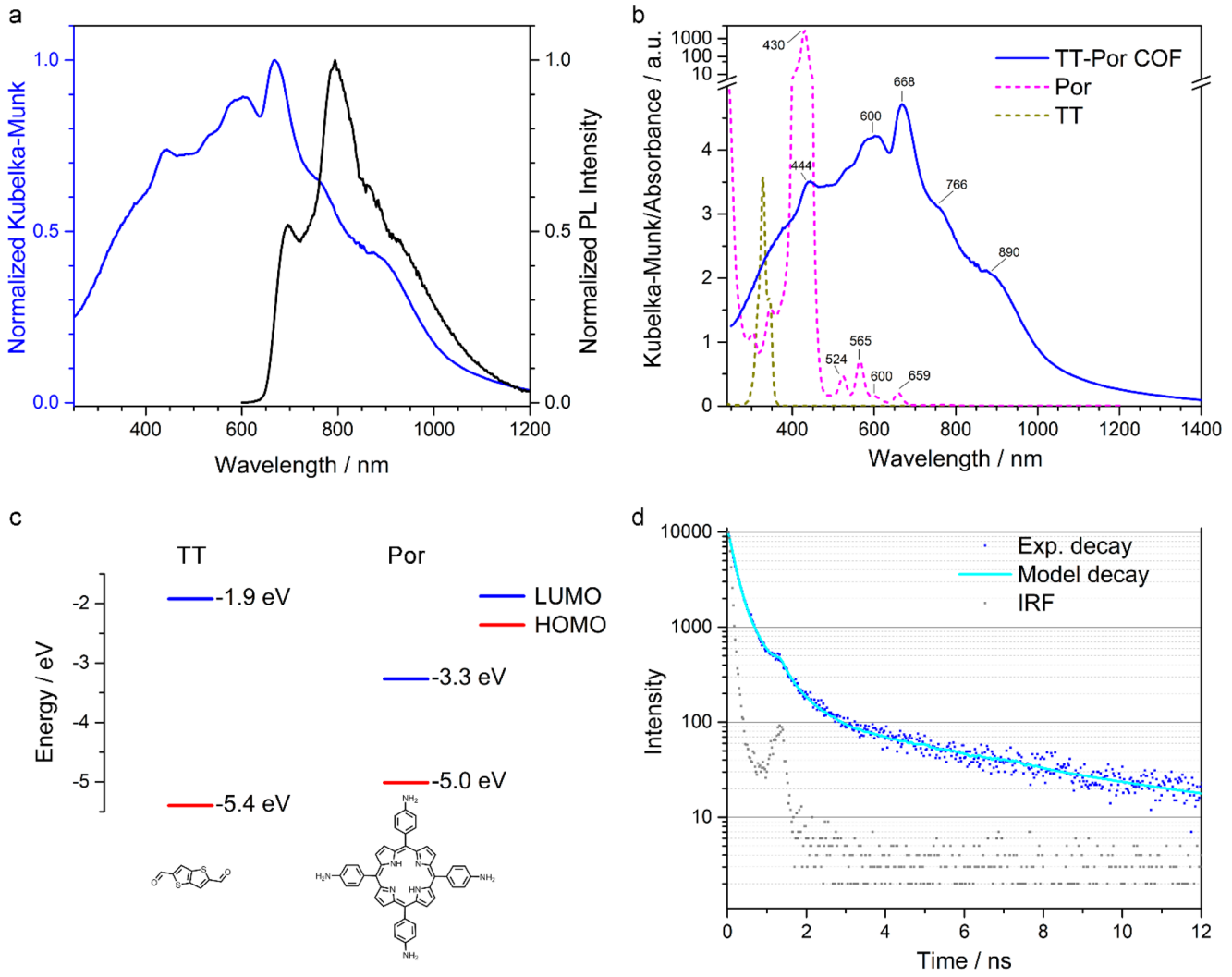

Figure 4. (a) Optical absorption (blue) spectrum of TT-Por COF measured as diffuse reflectance of the solid and converted with the Kubelka–Munk equation, and PL (λ_{exc} = 365 nm, black) spectrum of TT-Por COF, respectively. (b) Absorption spectra of the TT-Por COF measured in diffuse reflectance (blue) compared to the monomers (given in c; TT: dark yellow, dashed; Por: magenta, dashed) measured in diluted solution (50 μM, dioxane). (c) Relevant energy levels of the monomers with HOMO (red) and LUMO (blue), which were determined by combining differential pulse voltammetry measurements and UV–vis data. (d) Photoluminescence (PL) decay curve for TT-Por COF. The sample was illuminated at 378 nm with a pump fluence of ~0.99 nJ cm^{-2}; the emission was monitored at 800 nm (model decay in cyan).

attributed to the Q-bands of the porphyrin J-aggregate, together with the two shoulders at around 766 and 890 nm. The strong red-shift with respect to the monomer in solution indicates a large length scale of ordered J-aggregate-like staircase stacking, which is in good agreement with the PXRD data showing distinctly split peaks as well as the structural modeling. Furthermore, by comparing the COF absorption spectrum with neat porphyrin in powder form (see Figure S8a in the SI), a strong dominance of the porphyrin features is observed and considering the ratio of 2:1 between TT and porphyrin units, the TT absorption is small (overall <30% in the region of TT powder absorption). Direct comparison between COF and porphyrin solid monomer absorption shows no new absorption features arising in the COF and the overall absorption can be described, at least in terms of feature location, by a superposition of both neat material absorptions. However, as mentioned above, peak ratios strongly shift with much stronger absorption in the Q-bands due to the J-aggregate arrangement.[59] With little shift of the absorption features and no new ones emerging upon COF formation, we conclude that the aromatic system is essentially nonconjugated (Figure 4b), which can be explained by a 90° rotated phenylene ring between TT and the porphyrin core. We note that all absorption spectra from solid samples are obtained in reflection mode and converted with the Kubelka–Munk equation. The optical bandgap of the COF, estimated from the corresponding Tauc plot for direct and allowed transitions, is 1.25 eV (SI, Figure S9). With this small bandgap, TT-Por COF is an excellent candidate for a photoactive material, since its optical absorption covers almost the complete visible spectrum.

Upon excitation of the TT-Por COF at 365 nm, a distinct fluorescence occurs at 794 nm with a second smaller peak at 696 nm (Figure 4a, black). The position of the latter peak is possibly obscured by self-absorption of the COF. Comparing the emission of COF and aggregated monomers (see the SI, Figure S10), the spectral shape does not correlate to a superposition of the neat monomer emissions. The strong overlap between absorption and emission of the COF is not

DOI: 10.1021/jacs.8b08088
J. Am. Chem. Soc. 2018, 140, 16544–16552

clear but similar optical behavior has been observed for porphyrins in the literature before.[20−23,60,61]

Electrochemical measurements provide insights into the oxidation and reduction potentials of the electroactive linker molecules. In order to determine the exact energy level of the highest occupied molecular orbital (HOMO), differential pulse voltammetry (DPV) was applied in dilute solutions in which the samples exist as single molecules. Ferrocene was used as internal reference and a potential of $E(Fc/Fc^{+}) = -4.80$ eV vs E_{vac} was assumed.[62] The sum of the HOMO and the bandgap energy, which was obtained from the Tauc plot, yielded the position of the lowest unoccupied molecular orbital (LUMO) and the energy levels of the bandgap with $E_{HOMO}(TT) = -5.40$ eV, $E_{LUMO}(TT) = -1.92$ eV, $E_{HOMO}(Por) = -5.01$ eV, and $E_{LUMO}(Por) = -3.27$ eV (Figure 4c). We note that since the connecting building blocks rotate out of the plane (Figure 2b), overlap between the orbitals of the aromatic linker molecules is restricted, reducing the effective conjugation of the resulting COF as confirmed by UV−vis measurements.

Photoluminescence (PL) dynamics provide important information on the lifetime of the initially generated singlet. To determine the PL dynamics, time-correlated single photon counting (TCSPC) was applied using a pulsed 378 nm laser (see the SI for method). The PL decay of TT-Por COF was measured at 800 nm and the resulting histogram was fitted with the sum of three exponentials (see SI for full set of parameters). The long-time decay constant is 4.90 ns (Figure 4d) which is among the longest lifetimes for COF PL reported in the literature.[63,64] This decay time is somewhat shorter than that of the monomers in solution, which show PL decays on a time scale of 4 and 9 ns, as has been observed in the literature.[60] However, the pure solid starting materials TT and (**1**) exhibit average lifetimes of 1.12 and 0.67 ns, respectively (SI, Figure S14). Hence, the results show a significant increase of singlet lifetime within the COF compared to the neat solids, which we attribute to a stabilization of the singlet state within the well-defined spatial molecular arrangements within the COF lattice.

To investigate the influence of the TT building block on the excited state lifetimes, three additional porphyrin COFs were synthesized from compound **1** and different linear building blocks (for more details, see the SI, sections 4 and 5). As the first example, 2,5-dimethoxybenzene-1,4-dicarboxaldehyde (OMe) was used as bridging unit between the four-armed porphyrin molecules.[65] The PL decay of the resulting OMe-Por COF structure was analyzed by TCSPC and the lifetimes of the excited species were found to be merely the sum of the lifetimes of its two components, without any noticeable impact due to embedding in the COF lattice (for more information see the SI, section 7). As a second example COF-366 was chosen, formed by combining compound (**1**) with terephthalaldehyde (1P; for experimental details see the SI, section 2) as reported in the literature.[23] It showed a fluorescence lifetime of less than 1 ns, suggesting the occurrence of processes analogous to those within the starting materials. Comparing optical absorption and PXRD data between the three different COFs, TT-Por shows the strongest aggregation, as derived from the most pronounced red-shift of the optical absorption and splitting of PXRD peaks. This indicates that the extended lifetime of the fluorescent species within the TT-Por COF compared to its components is a result of the J-aggregate formation, allowing for a better delocalization of the singlet across the porphyrin units. This delocalization throughout the COF structure causes a stabilization of the excited species and prolonged lifetimes. With the weaker aggregation arising within the OMe-Por and COF-366 structures, singlets are more localized and hence resemble the behavior on solid monomers. As a result, no prolonged lifetimes of the excited species could be observed in these COFs.

CONCLUSION

In this study we have developed a new offset-stacked imine-linked COF comprising tetragonal porphyrin and linear thienothiophene building blocks, resulting in the formation of J-aggregate stacks of unprecedented spatial extension. This aggregation enables substantially prolonged lifetimes of the singlet excitons compared to the solid starting materials, as indicated by the PL dynamics. Hence, covalently embedding the chromophore building blocks in the COF forces the formation of aggregates and facilitates exciton delocalization throughout the framework as well as stabilization of the excited species. Through careful covalent framework design, this directed stacking arrangement could potentially be transferred to other chromophore systems as well, allowing for specific utilization of the aggregate benefits. This aggregation-based spectral tuning of (sustainable) chromophores can lead to materials with appealing bandgaps in the NIR region. Moreover, we believe that the insights gained from these well-defined model systems can be transferred to currently used organic photovoltaic devices and help to understand and optimize these systems. Specifically, the strong absorption of the TT-Por COF in the visible is desirable for harvesting a large fraction of the solar spectrum, and the prolonged singlet lifetime would be beneficial for charge separation and ultimately collecting the energy of these excitations. Applications in photovoltaics would require the design of appropriate heterojunctions providing efficient exciton diffusion and dissociation as well as efficient charge carrier transport.

Moreover, the solid COF matrix in which these J-aggregates are incorporated enables efficient molecular access through the porous framework for interactions with liquids and gases. This would allow valuable insights and open up a new basis for experiments with porphyrin aggregates without the need of aqueous environments and pH restrictions. Here, especially the close relation to molecules occurring in nature such as chlorophyll could be of interest, and possibly similar COFs enforcing J-aggregates can be built with metal-containing porphyrins. Thus, this type of COF could be used as a model system for biological, chemical, and medical applications. Recently, porphyrin aggregates have attracted great interest due to their increased two-photon absorption cross-section that can be used to selectively target tumor cells in human tissue with photodynamic therapy (PDT).[66−69] Due to the use of NIR light, high spatial resolution, deep tissue penetration depths (of around 2 cm) and selective excitation can be achieved, which is of great advantage in PDT.[1] Furthermore, this architecture could lead to new materials for the photodynamic inactivation of bacteria due to enhanced absorption by the enforced J-aggregate stacking of porphyrins within the COF.[70] The entire set of special features of such COFs, i.e., the high density of chromophores, intrinsic porosity and crystallinity, as well as intriguing optical characteristics, are expected to open a vast field of new opportunities where highly ordered aggregates yield new insights and functionalities.

DOI: 10.1021/jacs.8b08088
J. Am. Chem. Soc. 2018, 140, 16544−16552

■ ASSOCIATED CONTENT

Supporting Information

The Supporting Information is available free of charge on the ACS Publications website at DOI: 10.1021/jacs.8b08088.

Experimental methods, synthetic procedures, and additional structural and spectroscopic data (PDF)

■ AUTHOR INFORMATION

Corresponding Author

*bein@lmu.de

ORCID

Niklas Keller: 0000-0003-1581-072X
Dmitry Sharapa: 0000-0001-9510-9081
Himadri R. Soni: 0000-0002-2497-9351
Sabrina Rager: 0000-0002-3938-1790
Florian Auras: 0000-0003-1709-4384
Andreas C. Jakowetz: 0000-0001-7804-7210
Andreas Görling: 0000-0002-1831-3318
Timothy Clark: 0000-0001-7931-4659
Thomas Bein: 0000-0001-7248-5906

Present Address

¶(H.R.S.) School of Sciences, Indrashil University, Rajpur 382740, Kadi, Mehesana, India

Notes

The authors declare no competing financial interest.

■ ACKNOWLEDGMENTS

The authors are grateful for funding from the German Science Foundation (DFG; Research Cluster Nanosystems Initiative Munich (NIM), Priority Programme "Control of London Dispersion Interactions in Molecular Chemistry" (SPP 1807): TS 87/17-1) and from the Free State of Bavaria (Research Network "Solar Technologies go Hybrid"). The research leading to these results has received funding from the European Research Council under the European Union's Seventh Framework Programme (FP7/2007-2013)/ERC Grant Agreement No. 321339.

■ REFERENCES

(1) Shen, Y.; Shuhendler, A. J.; Ye, D.; Xu, J.-J.; Chen, H.-Y. Two-photon excitation nanoparticles for photodynamic therapy. *Chem. Soc. Rev.* **2016**, *45* (24), 6725−6741.

(2) Satake, A.; Kobuke, Y. Artificial photosynthetic systems: assemblies of slipped cofacial porphyrins and phthalocyanines showing strong electronic coupling. *Org. Biomol. Chem.* **2007**, *5* (11), 1679−1691.

(3) Kasha, M.; Rawls, H. R.; El-Bayoumi, M. A. The Exciton Model in Molecular Spectroscopy. *Pure Appl. Chem.* **1965**, *11*, 371−392.

(4) Wasielewski, M. R. Photoinduced electron transfer in supramolecular systems for artificial photosynthesis. *Chem. Rev.* **1992**, *92* (3), 435−461.

(5) Anderson, H. L. Building molecular wires from the colours of life: conjugated porphyrin oligomers. *Chem. Commun.* **1999**, No. 23, 2323−2330.

(6) Chen, L.; Yang, Y.; Guo, Z.; Jiang, D. Highly Efficient Activation of Molecular Oxygen with Nanoporous Metalloporphyrin Frameworks in Heterogeneous Systems. *Adv. Mater.* **2011**, *23* (28), 3149−3154.

(7) Chen, L.; Yang, Y.; Jiang, D. CMPs as Scaffolds for Constructing Porous Catalytic Frameworks: A Built-in Heterogeneous Catalyst with High Activity and Selectivity Based on Nanoporous Metalloporphyrin Polymers. *J. Am. Chem. Soc.* **2010**, *132* (26), 9138−9143.

(8) Li, Y.; Auras, F.; Löbermann, F.; Döblinger, M.; Schuster, J.; Peter, L.; Trauner, D.; Bein, T. A Photoactive Porphyrin-Based Periodic Mesoporous Organosilica Thin Film. *J. Am. Chem. Soc.* **2013**, *135*, 18513−18519.

(9) Luo, L.; Lin, C.-J.; Hung, C.-S.; Lo, C.-F.; Lin, C.-Y.; Diau, E. W.-G. Effects of potential shift and efficiency of charge collection on nanotube-based porphyrin-sensitized solar cells with conjugated links of varied length. *Phys. Chem. Chem. Phys.* **2010**, *12*, 12973−12977.

(10) Maiti, N. C.; Mazumdar, S.; Periasamy, N. J- and H-Aggregates of Porphyrin-Surfactant Complexes: Time-Resolved Fluorescence and Other Spectroscopic Studies. *J. Phys. Chem. B* **1998**, *102*, 1528−1538.

(11) Li, L.; Huang, Y.; Peng, J.; Cao, Y.; Peng, X. Highly responsive organic near-infrared photodetectors based on a porphyrin small molecule. *J. Mater. Chem. C* **2014**, *2* (8), 1372−1375.

(12) Martínez-Díaz, M. V.; de la Torre, G.; Torres, T. Lighting porphyrins and phthalocyanines for molecular photovoltaics. *Chem. Commun.* **2010**, *46*, 7090−7108.

(13) Scholes, G. D.; Fleming, G. R.; Olaya-Castro, A.; van Grondelle, R. Lessons from nature about solar light harvesting. *Nat. Chem.* **2011**, *3* (10), 763−74.

(14) Sundström, V.; Pullerits, T.; van Grondelle, R. Photosynthetic Light-Harvesting: Reconciling Dynamics and Structure of Purple Bacterial LH2 Reveals Function of Photosynthetic Unit. *J. Phys. Chem. B* **1999**, *103* (13), 2327−2346.

(15) van Grondelle, R. Excitation energy transfer, trapping and annihilation in photosynthetic systems. *Biochim. Biophys. Acta, Rev. Bioenerg.* **1985**, *811* (2), 147−195.

(16) Michel, H.; Deisenhofer, J. Relevance of the photosynthetic reaction center from purple bacteria to the structure of photosystem II. *Biochemistry* **1988**, *27* (1), 1−7.

(17) Jelley, E. E. Spectral Absorption and Fluorescence of Dyes in the Molecular State. *Nature* **1936**, *138*, 1009.

(18) Jelley, E. E. Molecular, Nematic and Crystal States of I: I-Diethyl–Cyanine Chloride. *Nature* **1937**, *139*, 631.

(19) Kasha, M. Energy Transfer Mechanisms and the Molecular Exciton Model for Molecular Aggregates. *Radiat. Res.* **1963**, *20* (1), 55−70.

(20) Egawa, Y.; Hayashida, R.; Anzai, J.-I. pH-Induced Interconversion between J-Aggregates and H-Aggregates of 5,10,15,20-Tetrakis(4-sulfonatophenyl)porphyrin in Polyelectrolyte Multilayer Films. *Langmuir* **2007**, *23* (26), 13146−13150.

(21) Kano, H.; Kobayashi, T. Time-resolved fluorescence and absorption spectroscopies of porphyrin J-aggregates. *J. Chem. Phys.* **2002**, *116* (1), 184.

(22) Ohno, O.; Kaizu, Y.; Kobayashi, H. J-aggregate formation of a water-soluble porphyrin in acidic aqueous media. *J. Chem. Phys.* **1993**, *99* (5), 4128.

(23) Wan, S.; Gándara, F.; Asano, A.; Furukawa, H.; Saeki, A.; Dey, S. K.; Liao, L.; Ambrogio, M. W.; Botros, Y. Y.; Duan, X.; Seki, S.; Stoddart, J. F.; Yaghi, O. M. Covalent Organic Frameworks with High Charge Carrier Mobility. *Chem. Mater.* **2011**, *23* (18), 4094−4097.

(24) Giovannetti, R. *The Use of Spectrophotometry UV-Vis for the Study of Porphyrins, Macro To Nano Spectroscopy*; InTech, 2012.

(25) Saptal, V.; Shinde, D. B.; Banerjee, R.; Bhanage, B. M. State-of-the-art catechol porphyrin COF catalyst for chemical fixation of carbon dioxide via cyclic carbonates and oxazolidinones. *Catal. Sci. Technol.* **2016**, *6* (15), 6152−6158.

(26) Liao, H.; Wang, H.; Ding, H.; Meng, X.; Xu, H.; Wang, B.; Ai, X.; Wang, C. A 2D porous porphyrin-based covalent organic framework for sulfur storage in lithium-sulfur batteries. *J. Mater. Chem. A* **2016**, *4* (19), 7416−7421.

(27) Lin, S.; Diercks, C. S.; Zhang, Y.-B.; Kornienko, N.; Nichols, E. M.; Zhao, Y.; Paris, A. R.; Kim, D.; Yang, P.; Yaghi, O. M.; Chang, C. J. Covalent organic frameworks comprising cobalt porphyrins for catalytic CO2 reduction in water. *Science* **2015**, *349* (6253), 1208−1213.

(28) Chen, X.; Addicoat, M.; Jin, E.; Zhai, L.; Xu, H.; Huang, N.; Guo, Z.; Liu, L.; Irle, S.; Jiang, D. Locking Covalent Organic Frameworks with Hydrogen Bonds: General and Remarkable Effects

DOI: 10.1021/jacs.8b08088
J. Am. Chem. Soc. 2018, 140, 16544−16552

on Crystalline Structure, Physical Properties, and Photochemical Activity. *J. Am. Chem. Soc.* **2015**, *137* (9), 3241−3247.
(29) Calik, M.; Auras, F.; Salonen, L. M.; Bader, K.; Grill, I.; Handloser, M.; Medina, D. D.; Dogru, M.; Löbermann, F.; Trauner, D.; Hartschuh, A.; Bein, T. Extraction of Photogenerated Electrons and Holes from a Covalent Organic Framework Integrated Heterojunction. *J. Am. Chem. Soc.* **2014**, *136* (51), 17802−17807.
(30) Feng, X.; Liu, L.; Honsho, Y.; Saeki, A.; Seki, S.; Irle, S.; Dong, Y.; Nagai, A.; Jiang, D. High-Rate Charge-Carrier Transport in Porphyrin Covalent Organic Frameworks: Switching from Hole to Electron to Ambipolar Conduction. *Angew. Chem., Int. Ed.* **2012**, *51* (11), 2618−2622.
(31) Xu, H.; Chen, X.; Gao, J.; Lin, J.; Addicoat, M.; Irle, S.; Jiang, D. Catalytic covalent organic frameworks via pore surface engineering. *Chem. Commun.* **2014**, *50* (11), 1292−1294.
(32) Hou, Y.; Zhang, X.; Sun, J.; Lin, S.; Qi, D.; Hong, R.; Li, D.; Xiao, X.; Jiang, J. Good Suzuki-coupling reaction performance of Pd immobilized at the metal-free porphyrin-based covalent organic framework. *Microporous Mesoporous Mater.* **2015**, *214*, 108−114.
(33) Huang, N.; Chen, X.; Krishna, R.; Jiang, D. Two-Dimensional Covalent Organic Frameworks for Carbon Dioxide Capture through Channel-Wall Functionalization. *Angew. Chem., Int. Ed.* **2015**, *54* (10), 2986−2990.
(34) Hou, Y.; Zhang, X.; Wang, C.; Qi, D.; Gu, Y.; Wang, Z.; Jiang, J. Novel Imine-linked Porphyrin Covalent Organic Frameworks with Good Adsorption Removing Property of RhB. *New J. Chem.* **2017**, *41*, 6145.
(35) Wang, K.; Qi, D.; Li, Y.; Wang, T.; Liu, H.; Jiang, J. Tetrapyrrole macrocycle based conjugated two-dimensional mesoporous polymers and covalent organic frameworks: From synthesis to material applications. *Coord. Chem. Rev.* **2017**.
(36) Feng, X.; Chen, L.; Dong, Y.; Jiang, D. Porphyrin-based two-dimensional covalent organic frameworks: synchronized synthetic control of macroscopic structures and pore parameters. *Chem. Commun.* **2011**, *47*, 1979−1981.
(37) Feng, X.; Liu, L.; Honsho, Y.; Saeki, A.; Seki, S.; Irle, S.; Dong, Y.; Nagai, A.; Jiang, D. High-Rate Charge-Carrier Transport in Porphyrin Covalent Organic Frameworks: Switching from Hole to Electron to Ambipolar Conduction. *Angew. Chem., Int. Ed.* **2012**, *51*, 2618−2622.
(38) Jin, S.; Ding, X.; Feng, X.; Supur, M.; Furukawa, K.; Takahashi, S.; Addicoat, M.; El-Khouly, M. E.; Nakamura, T.; Irle, S.; Fukuzumi, S.; Nagai, A.; Jiang, D. Charge Dynamics in A Donor-Acceptor Covalent Organic Framework with Periodically Ordered Bicontinuous Heterojunctions. *Angew. Chem., Int. Ed.* **2013**, *52*, 2017−2021.
(39) Jin, S.; Furukawa, K.; Addicoat, M.; Chen, L.; Takahashi, S.; Irle, S.; Nakamura, T.; Jiang, D. Large pore donor-acceptor covalent organic frameworks. *Chem. Sci.* **2013**, *4*, 4505−4511.
(40) Kandambeth, S.; Shinde, D. B.; Panda, M. K.; Lukose, B.; Heine, T.; Banerjee, R. Enhancement of Chemical Stability and Crystallinity in Porphyrin-Containing Covalent Organic Frameworks by Intramolecular Hydrogen Bonds. *Angew. Chem., Int. Ed.* **2013**, *52*, 13052−13056.
(41) Neti, V. S. P. K.; Wu, X.; Deng, S.; Echegoyen, L. Synthesis of a phthalocyanine and porphyrin 2D covalent organic framework. *CrystEngComm* **2013**, *15*, 6892−6895.
(42) Spitler, E. L.; Koo, B. T.; Novotney, J. L.; Colson, J. W.; Uribe-Romo, F. J.; Gutierrez, G. D.; Clancy, P.; Dichtel, W. R. A 2D Covalent Organic Framework with 4.7-nm Pores and Insight into Its Interlayer Stacking. *J. Am. Chem. Soc.* **2011**, *133*, 19416−19421.
(43) Zhou, W.; Wu, H.; Yildirim, T. Structural stability and elastic properties of prototypical covalent organic frameworks. *Chem. Phys. Lett.* **2010**, *499* (1−3), 103−107.
(44) Ascherl, L.; Sick, T.; Margraf, J. T.; Lapidus, S. H.; Calik, M.; Hettstedt, C.; Karaghiosoff, K.; Döblinger, M.; Clark, T.; Chapman, K. W.; Auras, F.; Bein, T. Molecular docking sites designed for the generation of highly crystalline covalent organic frameworks. *Nat. Chem.* **2016**, *8* (4), 310−316.
(45) Auras, F.; Ascherl, L.; Hakimioun, A. H.; Margraf, J. T.; Hanusch, F. C.; Reuter, S.; Bessinger, D.; Döblinger, M.; Hettstedt, C.; Karaghiosoff, K.; Herbert, S.; Knochel, P.; Clark, T.; Bein, T. Synchronized Offset Stacking: A Concept for Growing Large-Domain and Highly Crystalline 2D Covalent Organic Frameworks. *J. Am. Chem. Soc.* **2016**, *138*, 16703−16710.
(46) Keller, N.; Bessinger, D.; Reuter, S.; Calik, M.; Ascherl, L.; Hanusch, F. C.; Auras, F.; Bein, T. Oligothiophene-Bridged Conjugated Covalent Organic Frameworks. *J. Am. Chem. Soc.* **2017**, *139*, 8194−8199.
(47) Bessinger, D.; Ascherl, L.; Auras, F.; Bein, T. Spectrally Switchable Photodetection with Near-Infrared-Absorbing Covalent Organic Frameworks. *J. Am. Chem. Soc.* **2017**, *139* (34), 12035−12042.
(48) Kresse, G.; Furthmüller, J. Efficiency of ab-initio total energy calculations for metals and semiconductors using a plane-wave basis set. *Comput. Mater. Sci.* **1996**, *6* (1), 15−50.
(49) Perdew, J. P.; Burke, K.; Ernzerhof, M. Generalized Gradient Approximation Made Simple. *Phys. Rev. Lett.* **1996**, *77* (18), 3865−3868.
(50) Grimme, S.; Antony, J.; Ehrlich, S.; Krieg, H. A consistent and accurate ab initio parametrization of density functional dispersion correction (DFT-D) for the 94 elements H-Pu. *J. Chem. Phys.* **2010**, *132* (15), 154104.
(51) Grimme, S.; Ehrlich, S.; Goerigk, L. Effect of the damping function in dispersion corrected density functional theory. *J. Comput. Chem.* **2011**, *32* (7), 1456−1465.
(52) Dewar, M. J. S.; Thiel, W. Ground states of molecules. 38. The MNDO method. Approximations and parameters. *J. Am. Chem. Soc.* **1977**, *99* (15), 4899−4907.
(53) Dewar, M. J. S.; Yuan, Y. C. AM1 parameters for sulfur. *Inorg. Chem.* **1990**, *29* (19), 3881−3890.
(54) Thiel, W.; Voityuk, A. A. Extension of MNDO to d Orbitals: Parameters and Results for the Second-Row Elements and for the Zinc Group. *J. Phys. Chem.* **1996**, *100* (2), 616−626.
(55) Dewar, M. J. S.; Zoebisch, E. G.; Healy, E. F.; Stewart, J. J. P. Development and use of quantum mechanical molecular models. 76. AM1: a new general purpose quantum mechanical molecular model. *J. Am. Chem. Soc.* **1985**, *107* (13), 3902−3909.
(56) Winget, P.; Horn, A. H. C.; Selçuki, C.; Martin, B.; Clark, T. AM1* parameters for phosphorus, sulfur and chlorine. *J. Mol. Model.* **2003**, *9* (6), 408−414.
(57) Hennemann, M.; Clark, T. EMPIRE: a highly parallel semiempirical molecular orbital program: 1: self-consistent field calculations. *J. Mol. Model.* **2014**, *20* (7), 2331.
(58) Margraf, J. T.; Hennemann, M.; Meyer, B.; Clark, T. EMPIRE: a highly parallel semiempirical molecular orbital program: 2: periodic boundary conditions. *J. Mol. Model.* **2015**, *21* (6), 144.
(59) Zimmermann, J.; Siggel, U.; Fuhrhop, J.-H.; Röder, B. Excitonic Coupling between B and Q Transitions in a Porphyrin Aggregate. *J. Phys. Chem. B* **2003**, *107* (25), 6019−6021.
(60) Verma, S.; Ghosh, A.; Das, A.; Ghosh, H. N. Ultrafast Exciton Dynamics of J- and H-Aggregates of the Porphyrin-Catechol in Aqueous Solution. *J. Phys. Chem. B* **2010**, *114* (25), 8327−8334.
(61) Maiti, N. C.; Mazumdar, S.; Periasamy, N. J- and H-Aggregates of Porphyrin−Surfactant Complexes: Time-Resolved Fluorescence and Other Spectroscopic Studies. *J. Phys. Chem. B* **1998**, *102* (9), 1528−1538.
(62) Frost, J. M.; Faist, M. A.; Nelson, J. Energetic Disorder in Higher Fullerene Adducts: A Quantum Chemical and Voltammetric Study. *Adv. Mater.* **2010**, *22* (43), 4881−4884.
(63) Jin, S.; Furukawa, K.; Addicoat, M.; Chen, L.; Takahashi, S.; Irle, S.; Nakamura, T.; Jiang, D. Large pore donor-acceptor covalent organic frameworks. *Chem. Sci.* **2013**, *4* (12), 4505−4511.
(64) Auras, F.; Ascherl, L.; Hakimioun, A. H.; Margraf, J. T.; Hanusch, F. C.; Reuter, S.; Bessinger, D.; Döblinger, M.; Hettstedt, C.; Karaghiosoff, K.; Herbert, S.; Knochel, P.; Clark, T.; Bein, T. Synchronized Offset Stacking: A Concept for Growing Large-Domain

DOI: 10.1021/jacs.8b08088
J. Am. Chem. Soc. 2018, 140, 16544−16552

and Highly Crystalline 2D Covalent Organic Frameworks. *J. Am. Chem. Soc.* **2016**, *138* (51), 16703−16710.
(65) Kandambeth, S.; Shinde, D. B.; Panda, M. K.; Lukose, B.; Heine, T.; Banerjee, R. Enhancement of Chemical Stability and Crystallinity in Porphyrin-Containing Covalent Organic Frameworks by Intramolecular Hydrogen Bonds. *Angew. Chem., Int. Ed.* **2013**, *52* (49), 13052−13056.
(66) Secret, E.; Maynadier, M.; Gallud, A.; Chaix, A.; Bouffard, E.; Gary-Bobo, M.; Marcotte, N.; Mongin, O.; El Cheikh, K.; Hugues, V.; Auffan, M.; Frochot, C.; Morère, A.; Maillard, P.; Blanchard-Desce, M.; Sailor, M. J.; Garcia, M.; Durand, J.-O.; Cunin, F. Two-Photon Excitation of Porphyrin-Functionalized Porous Silicon Nanoparticles for Photodynamic Therapy. *Adv. Mater.* **2014**, *26* (45), 7643−7648.
(67) Mauriello-Jimenez, C.; Henry, M.; Aggad, D.; Raehm, L.; Cattoen, X.; Wong Chi Man, M.; Charnay, C.; Alpugan, S.; Ahsen, V.; Tarakci, D. K.; Maillard, P.; Maynadier, M.; Garcia, M.; Dumoulin, F.; Gary-Bobo, M.; Coll, J.-L.; Josserand, V.; Durand, J.-O. Porphyrin- or phthalocyanine-bridged silsesquioxane nanoparticles for two-photon photodynamic therapy or photoacoustic imaging. *Nanoscale* **2017**, *9* (43), 16622−16626.
(68) Mauriello-Jimenez, C.; Croissant, J.; Maynadier, M.; Cattoen, X.; Wong Chi Man, M.; Vergnaud, J.; Chaleix, V.; Sol, V.; Garcia, M.; Gary-Bobo, M.; Raehm, L.; Durand, J.-O. Porphyrin-functionalized mesoporous organosilica nanoparticles for two-photon imaging of cancer cells and drug delivery. *J. Mater. Chem. B* **2015**, *3* (18), 3681−3684.
(69) Biswas, S.; Ahn, H.-Y.; Bondar, M. V.; Belfield, K. D. Two-Photon Absorption Enhancement of Polymer-Templated Porphyrin-Based J-Aggregates. *Langmuir* **2012**, *28* (2), 1515−1522.
(70) Hynek, J.; Zelenka, J.; Rathouský, J.; Kubát, P.; Ruml, T.; Demel, J.; Lang, K. Designing Porphyrinic Covalent Organic Frameworks for the Photodynamic Inactivation of Bacteria. *ACS Appl. Mater. Interfaces* **2018**, *10* (10), 8527−8535.

DOI: 10.1021/jacs.8b08088
J. Am. Chem. Soc. 2018, 140, 16544−16552